Antiphase states of sub-nanosecond Cr,Yb:YAG microchip self-Q-switched multimode laser

Jun Dong*, Akira Shirakawa, and Ken-ichi Ueda
Institute for Laser Science, University of Electro-Communications, 1-5-1 Chofugaoka, Chofu, Tokyo 182-8585, Japan

Abstract

The antiphase states were observed experimentally in a laser-diode pumped sub-nanosecond microchip Cr,Yb:YAG self-Q-switched multimode laser which is resulted from the spatial hole burning effect. The stable two-mode, and three-mode oscillation are obtained with the increase of the pump power ratio. The modified multimode rate equations including the spatial hole-burning effect in the active medium and the non-linear absorption of the saturable absorber is proposed. The numerical simulations of the antiphase dynamics of such laser are in good agreement with the experimental data and the antiphase dynamics was explained by the evolution of the inversion population and the bleaching and recovery of the inversion population of the saturable absorber.

Keywords: Diode-pumped laser, passively Q-switched, antiphase state, spatial hole-buring

1. INTRODUCTION

The complicated behaviors of multimode laser have been well known from the early dates of laser experiments. Recently complex multimode lasers dynamics have been revisited as an interesting subject for the study of nonlinear dynamics in the optical systems. The nonlinear dynamics in multimode lasers include chaos and nonlinear mode coupling effect such as antiphase dynamics, and so on. The antiphase state was first described by Hadley and Beasley circuits containing N coupled Jesephson junctions, which is periodic in time with each oscillator having precisely the same waveform. However, each oscillator is shifted by $1/N$ of a period from its neighbor[1]. Similar dynamics were observed in the output of a multimode laser with an intracavity doubling crystal [2], and multimode lasers with gain or loss modulations[3]. In addition to being interesting for fabrication of compact integrated optical devices, microchip lasers are interesting systems for nonlinear dynamics studies. Indeed, microchip solid-state lasers are widely used as lasers for studying the nonlinear effects such as chaos and antiphase dynamics[3-8]. It has been demonstrated that antiphse states can be used as a method for secure information encoding and transmission[9]. There are many reports on the antiphase states of continuous wave microchip lasers[3-6] and some reports on the passively Q-switched Nd:YAG lasers with Cr^{4+} [7] as saturable absorber and Yb:YAG laser with semiconductor saturable absorber mirror (SESAM) as saturable absorber, however, there is no such report on the monolithic microchip passively Q-switched laser. Laser-diode-pumped passively Q-switched microchip solid-state lasers capable of delivering high peak power (several tens kW) at high repetition rate and nanosecond or sub-nanosecond pulse width can not only be potentially used in micro-machine, remote sensing, target ranging, microsurgery, pollution monitoring, and so on [10-14], but also can be as an compact resource for studying of the nonlinear dynamics. Recently, the sub-nanosecond laser pulses were obtained in a laser-diode-pumped Cr,Yb:YAG microchip laser[15], the stable antiphase states were observed in such a very compact multimode laser source. In this paper, we report the experimental results of antiphase dynamics in laser-diode-pumped Cr,Yb:YAG microchip self-Q-switched laser, the classical antiphase states were observed in two-mode oscillation regime and quasi- antiphase states were observed in the three-modes oscillations regime. The modified multimode laser rate equations were proposed including the cross-saturation effect due to the spatial hole-burning effect and the nonlinear absorption effect of the Cr^{4+} saturable absorber in the Cr,Yb:YAG crystal. The numerical solution of the rate equations was obtained and the antiphase dynamics of Cr,Yb:YAG laser at two-mode oscillation and the three-mode oscillation were reproduced. The numerical solutions are in good agreement with the experimental data.

Optoelectronic Materials and Devices for Optical Communications, edited by Shinji Tsuji, Jens Buus, Yi Luo, Proc. of SPIE Vol. 6020, 60201C, (2005) · 0277-786X/05/$15 · doi: 10.1117/12.634969

2. EXPERIMENTS

The schematic of the laser diode pumped microchip Cr,Yb:YAG self-Q-switched laser experimental setup is shown in Fig. 1. A plane-plane geometry 1 mm-thickness Cr,Yb:YAG crystal doped with 10 at.% Yb and 0.025 at.% Cr was used as a laser resonator. The planar rear surface is coated for high transmission (>90%) at 940 nm and total reflection (>97%) at 1030 nm. The planar front surface serving as output coupler is coated for 85% reflection at 1030 nm and total reflection (>98%) at 940 nm. A 2-W fiber-coupled 937.5 nm laser diode with a core diameter of 102 μm and numerical aperture of 0.15 was used as the pump source. The coupling optics (two focus lens with focus length of 8 mm) was used to focus the pump beam into the crystal rear surface. After the coupling optics, there is about 92% pump power incident on the Cr,Yb:YAG crystal and the pump light spot in Cr,Yb:YAG is about 100 μm in diameter. The Cr,Yb:YAG laser operation was performed at room temperature without cooling Cr,Yb:YAG crystal. The Q-switched pulses were recorded by using a fiber-coupled InGaAs photodiode (Model DSC40S from Discovery Semiconductor) with a bandwidth of 16 GHz, and a Tektronix TDS7704B digital phosphor oscilloscope of 7 GHz sampling rate in the single-shot mode. The laser spectrum was analyzed by using an ANDO AQ6317 optical spectrum analyzer. The laser output beam profile near the output coupler and far field was monitored by using the CCD camera, the beam diameter and beam quality M^2 can be determined. In order to study the dynamics of different sets of modes separately and make sure the detected signal is one mode of the solitary laser, a monochromator was used and the center wavelength of each mode was set to the peak position of each mode. The intensity waveforms of the total and a specific mode are detected with the photodiode detector and a fast digital oscilloscope simultaneously.

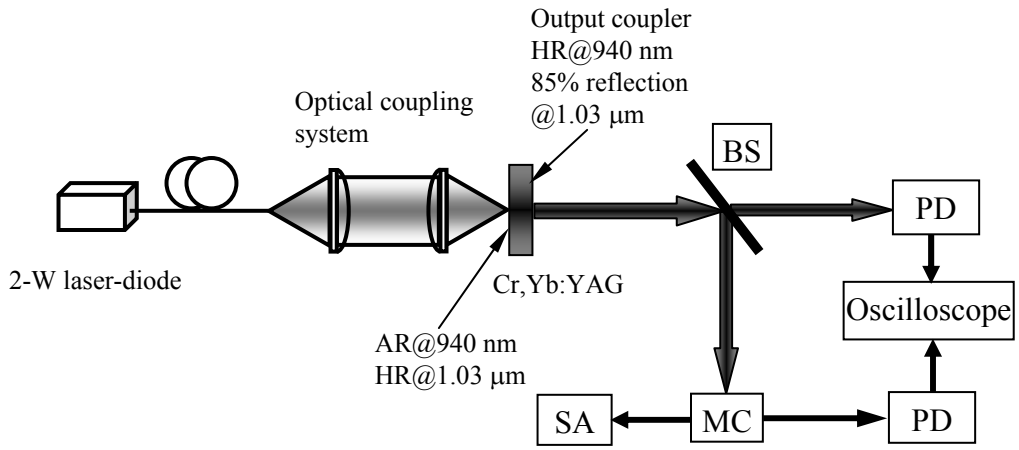

Figure 1: The schematic of the laser-diode-pumped microchip Cr,Yb:YAG self-Q-switched laser, BS, beam splitter; PD, Photodiode; MC, Monochromator; SA, Spectrum analyzer.

3. RESULTS AND DISCUSSION

The Q-switched pulses were observed when the absorbed pump power is above 680 mW, the minimum pulse width (FWHM) of 440 ps was obtained at absorbed pump power of 1500 mW and the repetition rate extends from several hundred Hz to 6.6 kHz with pump power. The output laser has a good TEM_{00} transverse intensity profile and near-diffraction-limited beam with M^2 of 1.17. The maximum average output power is 156 mW and the pulse energy is 23.5 μJ when the absorbed pump power is 1520 mW. The maximum peak power is over 53 kW. The laser spectrum of this self-Q-switched laser is longitudinal multimode (around 1030 nm) oscillation, the evolution of the self-Q-switched laser spectrum at different absorbed pump power is shown in Fig. 2. The wavelength of each mode shifts to the longer wavelength with increase of the absorbed pump power, this is caused by the increase of the temperature of the gain medium with increase of the absorbed pump power, the heat generated inside the gain medium increases, the emission spectrum of Yb:YAG crystal shifts to the longer wavelength with increase of the temperature as indicated in Ref. [16]. The number of lasing modes increases with the absorbed pump power. There is two-mode oscillation when the power is above threshold and w (ration of the absorbed pump power to the absorbed pump power threshold) is below 1.4. A third mode becomes active when the w is between 1.44 and 2. A fourth and fifth mode appears when w is 2.1 and w is 2.23, respectively, as shown in Fig. 2. But the intensity of the fourth-mode and fifth-mode is so weak that the forth-

mode and fifth-mode can be treated as chaos comparing to the other three main oscillation modes. Further increase of the absorbed pump power does not change the Q-switched laser spectrum. The separation of each frequency under different pump power is about 0.29 nm, the linewidth at each frequency is measured to be 0.02 nm. According to the laser resonator theory[17], the separation of the longitudinal modes in a laser cavity is given by $\Delta\lambda = \frac{\lambda^2}{2L_c}$, where L_c is the optical length of the resonator. For the 1 mm Cr,Yb:YAG planar-parallel resonator studied here, $\Delta\lambda$ was calculated to be 0.2915 nm with the laser wavelength of 1030 nm, the experimental data of the space between each mode is in good agreement with the theory prediction.

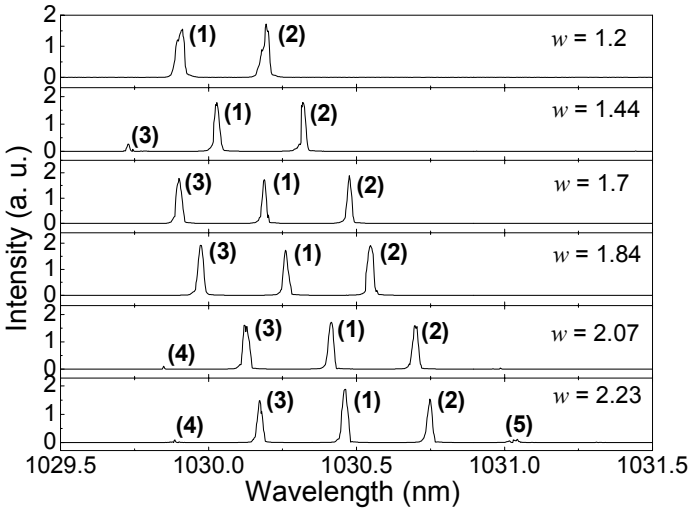

Figure 2: The evolution of the laser spectra around 1030 nm of Cr,Yb:YAG self-Q-switched laser with the absorbed pump power. The resolution of the measurement is 0.01 nm. The number in the bracket indicates the laser mode.

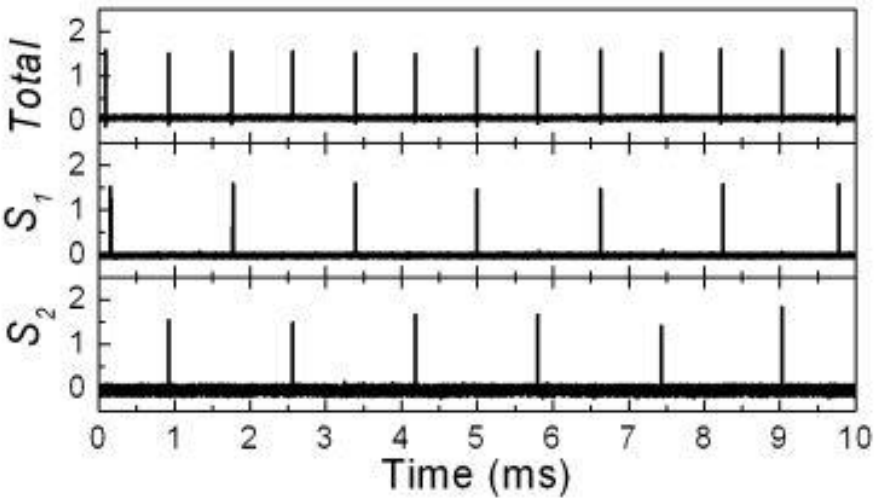

Figure 3: The total output pulse train and the output pulse trains of each mode of self-Q-switched Cr,Yb:YAG two-mode oscillation exhibiting the classic antiphase dynamics when the pump power ratio, $w = 1.2$.

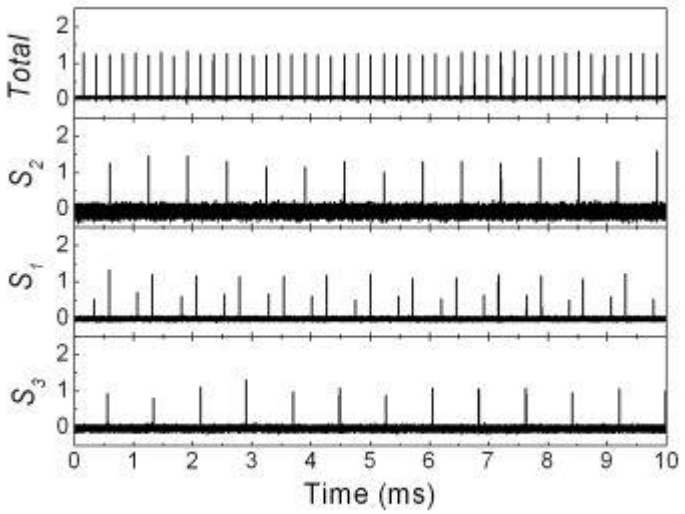

(a)

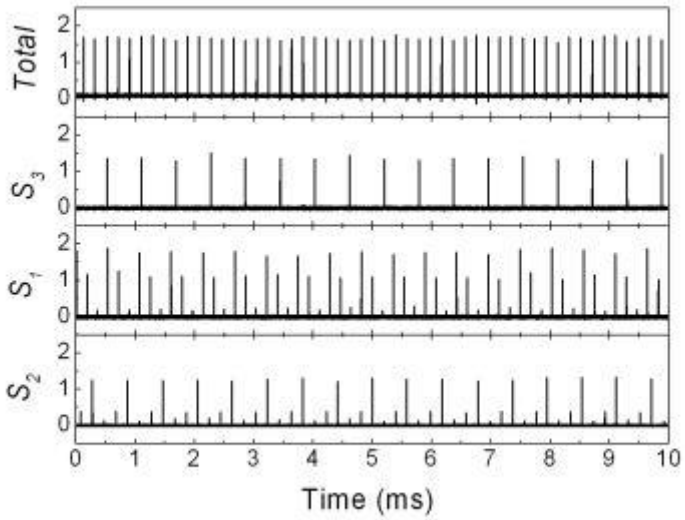

(b)

Figure 4: The total output pulse train and the output pulse trains of each mode of self-Q-switched Cr,Yb:YAG three-mode oscillation exhibiting the quasi- antiphase dynamics when the pump power ratio, (a) $w = 1.7$, (b) $w = 1.85$.

The antiphase dynamics of the self-Q-switched Cr,Yb:YAG multimode laser was studied experimentally by measuring the contribution of each mode to the total output intensity. The measured pulse trains of each mode and the total output laser can identify the temporal behavior of the multimode laser within the antiphase regime. A typical example of the measured pulse train of self-Q-switched two-mode laser and the pulse trains of each mode are shown in Fig. 3 when the pump power ratio, $w = 1.2$. The two modes oscillate nearly the same intensity. The two modes show period-1 pulsations with almost the same repetition frequency of 650 Hz, the total pulse repetition frequency, however, is 1.3 kHz, which is two times of that for each mode. Comparing the total pulse repetition frequency with those of each mode, each mode is shifted from the next mode by about 1/2 of the period. This shows that the two modes oscillation in opposite phase – the maximum of one mode coincide with the minimum of the other mode, the classic antiphase state. The antiphase state of this two-mode oscillation of microchip Cr,Yb:YAG laser is caused by the cross-saturation mechanism due to the spatial

hole burning coupling the modes via population gratings and the nonlinear absorption of the Cr^{4+} saturable absorber, the same as those reported by other researchers[7]. As soon as the pump power was increased up to the three-mode regime, in which the third lasing mode began to oscillate, the mode oscillation dynamics changes, and the intensity pulsations occur of the first mode with the highest gain characterized by two pulses as a group, which is different from those in two modes regime, as shown in Fig. 4, the ratio of the pump power, w = 1.7. The pulses of each mode are shifted from the next mode by 1/3 of the period of each mode and also display classic antiphase dynamics. As the pump power is further increased and the Q-switched laser is still in the three-mode oscillation regime, the corresponding output pulses of the first mode and second mode consist of two pulses, as shown in Fig. 4. In this three-mode oscillation regime, the maximum output intensity of the first mode still corresponds the quiescent states in other modes and still displays antiphase dynamics. Actually, antiphase dynamics need not to be periodic in each mode, and they can undergo bifurcation sequences. At the same time the oscillation repetition frequency of first and second modes are nearly the same as that of the total output pulse. The third mode oscillation repetition frequency is about 1/3 of the total output pulse. As the pump power is increased further, a fourth mode appears (as shown in Fig. 2) and the repetition frequency increases, the period of the first three modes is nearly the same as those displaying in the three-mode regime, the fourth mode can be treated as a chaotic oscillation because the intensity of this mode is very small comparing to the first three modes. It should be noted that the phases of the intensity pulses of individual modes are different and give rise to self-organized antiphase dynamics.

Taking the cross-saturation dynamics that is due to the spatial hole-burning effect into account [18], the modified rate equations for passively Q-switched multimode laser of N longitudinal modes with the same transverse mode structure including the nonlinear absorption of the saturable absorber are introduced as follows:

$$\frac{dn_0}{dt} = w - n_0 - \sum_{i=1}^{N} \gamma_i \left(n_0 - \frac{n_i}{2} \right) \phi_i \tag{1}$$

$$\frac{dn_i}{dt} = \gamma_i n_0 \phi_i - n_i \left(1 + \sum_{i=1}^{N} \gamma_i \phi_i \right) \tag{2}$$

$$\frac{d\phi_i}{dt} = K \left[\left(\gamma_i \left(n_0 - \frac{n_i}{2} \right) - 1 - 2\left(\delta_1 N_g - \delta_2 \left(N_0 - N_g \right) \right) l \right) \phi_i + \varepsilon n_0 \right] \tag{3}$$

$$\frac{dN_g}{dt} = \left(N_0 - N_g \right) \xi - \delta_1 N_g \sum_{i=1}^{N} \phi_i \tag{4}$$

with i = 1, …, N. In the Eq. (1 - 4), time is normalized to the fluorescence lifetime τ of gain medium, Cr,Yb:YAG; w is the relative pump rate normalized to the first-lasing-mode absorbed pump power threshold; n_0 is the space average of the population inversion density normalized to the first-lasing-mode threshold population inversion density, n_i is the normalized Fourier components of the population inversion density for the i-th mode normalized to the fist-lasing-mode threshold population inversion density, which can described as follows:

$$n_0 = \frac{1}{L_c} \int_0^{L_c} n(z,t) dz \tag{5}$$

$$n_i = \frac{2}{L_c} \int_0^{L_c} n(z,t) \cos(2k_i z) dz \tag{6}$$

where k_i is the wave number of mode i and L_c is the length of the cavity filled with active medium; ϕ_i is the normalized photon density, $\gamma_i \le 1$ is the relative gain with respect to the first lasing mode, $K = \tau / \tau_c$ is the lifetime ratio of the fluorescence lifetime of the gain medium and the photon lifetime inside the laser cavity, l is the length of the saturable absorber, ε is the spontaneous emission coefficient, δ_1 and δ_2 are the ratio of the ground absorption cross section and the excited state absorption cross section of Cr^{4+} saturable absorber to the stimulated emission cross section of the gain medium of Yb^{3+}, respectively. N_g, N_0 are the population inversion density and the total population density of Cr^{4+} saturable absorber normalized to the first-lasing-mode threshold. ξ is the ratio of the fluorescence lifetime of gain medium to the lifetime of the saturable absorber.

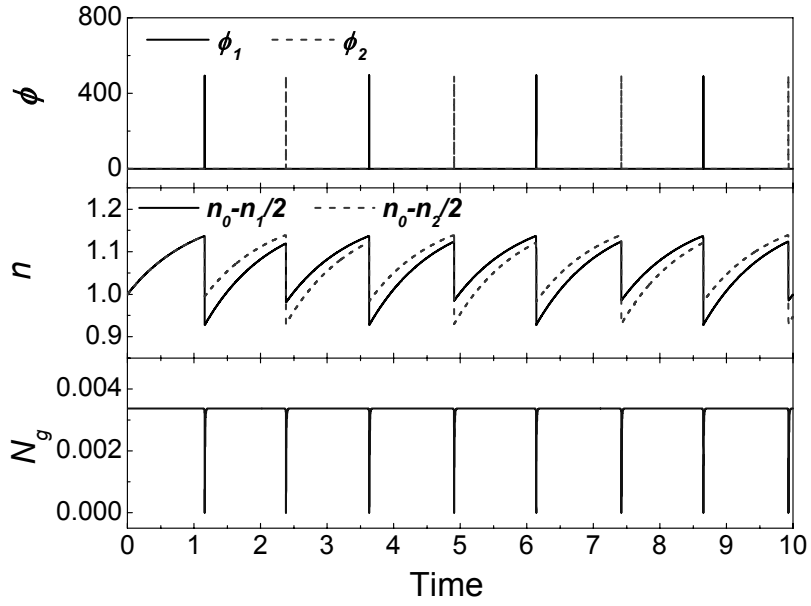

Figure 5: Numerical simulation of the pulse sequences, the population inversion of each mode and the population inversion of the saturable absorber for two-mode antiphase dynamics when the pump power ratio, $w = 1.2$.

Table 1 The parameters of Cr,Yb:YAG used in the numerical simulations [19]

Parameters	Value
σ	2.5×10^{-20} cm^2
σ_g	4.6×10^{-18} cm^2
σ_e	8.2×10^{-19} cm^2
τ	584 μs
τ_g	3.4 μs
K	1.5×10^{7}
N_0	3.37×10^{-3}
δ_1	200.87
δ_2	35.7
l	1 mm
ξ	172
ε	1.2×10^{-7}

Because the gain spectrum of Yb^{3+} in YAG crystal is broad (about 9 nm at room temperature [16]) enough as comparing with the longitudinal mode space (0.3 nm), the gain, loss and spontaneous emission rate are assumed to be the same for all modes in the following numerical simulations. A typical numerical example of the population inversion density of the saturable absorber and the population inversion density of two modes, n_0-n_1/2, n_0-n_2/2, and the photon density for two-mode oscillation is shown in Fig. 5, the pump rate $w = 1.2$, $\gamma_1 = 1$, $\gamma_2 = 0.99$, the other laser parameters [19] used in numerical calculations are listed in Table 1. ϕ_1 and ϕ_2 are the photon density of the two modes, respectively. The n_0-n_1/2 value in the figure is the population inversion for the first-mode oscillation and n_0-n_2/2 value is the population inversion for the second-mode oscillation. N_g is the inversion population of the saturable absorber. This numerical solution of two-mode oscillation is quite similar to the experimental result shown in Fig. 3. The maximum output intensity in one

mode is shifted 1/2 period of the repetition frequency from that of the other mode, which shows a classic antiphase state. The antiphase states was reproduced in the numerical calculations irrespective of the initial conditions for the mode intensities and gains, the antiphse state is generally existing at the two-mode oscillation regime. The mechanics of the alternative antiphase pulse oscillation of Cr,Yb:YAG self-Q-switched laser under continuous-wave pumping can be explained from Fig. 5 as follows [3]. The time interval between the pulses is governed by the buildup time of the population inversion n to reach the threshold value, pulse the growth time of the photon density ϕ (which too short to be considered comparing with the buildup time of the population inversion under continuous-wave pumping) after n exceeds the threshold. Under the continuous-wave pumping, the first mode of highest gain will reach the threshold first, and the second mode is suppressed to oscillate. Therefore, the decrease of the population inversion n_0-n_1/2 of the first mode, just after the oscillation, is more significant than that of n_0-n_2/2 for the second mode. Then, the recovery time of the population inversion to its threshold value is shorter for the second mode than for the first mode, and the second mode oscillation suppresses the first mode. The laser pulses of two-mode oscillate alternatively under the continuous-wave pumping and the nonlinear absorption of the saturable absorber, the delay time of each mode is determined by the nonlinear absorption of the saturable absorber. Similar antiphase behaviors of two-mode oscillation have been obtained generally for appropriate parameter w from 1.01 to 1.4. The numerical simulation of the population inversion density of the saturable absorber and the population inversion density of three modes, n_0-n_1/2, n_0-n_2/2, n_0-n_3/2 and the photon density for the three-mode oscillations with $\gamma_1 = 1$, $\gamma_2 = 0.99$, $\gamma_3 = 0.98$ under different pumping power ratio are showing in Fig. 6, which is similar to the experimental results shown in Fig. 4. The evolution of the inversion population density with time shows that the inversion population of three modes increases with time under the continuous-wave pumping, the first mode with highest gain reaches the threshold first, and suppresses the other modes oscillations. Then the saturable absorption was bleached under the highest gain of the first mode, the Q-switched pulse of the first mode was developed and the population inversion of the gain was depleted drastically for the first mode comparing to the other modes. The inversion population of the three modes increases with the continuous-wave pumping, the inversion population of the second mode will reach the threshold first because the final state inversion population is higher than that for the first- and third- mode, then the oscillation of the first- and third- mode oscillation was suppressed, the laser pulse of the second-mode was released, the inversion population of the second-mode, n_0-n_2/2 depletes significantly comparing to the third- and first- mode, at this time the third mode has the highest low state inversion population, and reaches the threshold first comparing to the first- and second- mode, the laser pulse of the third mode was released. Three modes oscillate alternatively; each mode shifts 1/3 of the period from the other and shows the typical antiphase dynamics. The antiphase dynamics of three modes dose not change with the increase of the pump power, however, the time interval between the pulses will be shortened with the increase of the pump power, as shown in Fig. 6. The time interval between each pulse for the total output is governed by the bleaching and recovery time of the population inversion of the Cr^{4+} saturable absorber. There are some discrepancies between the experimental results of the measured pulse trains of first-mode, second-mode and the numerical calculations for three-mode oscillation comparing Fig. 4 with Fig. 6. We assumed that the total loss of the cavity for each mode is the same during the numerical calculations, however, the loss for each mode is different in the experiments, and the mode oscillation becomes complicated with the pump power as shown in Fig. 4, there is two-pulse as a group for the first-mode oscillation when the pump power ratio is 1.7, there is two-pulse as a group for the first-mode, second-mode when the pump power ratio is 1.85. Uniformly distributed pump power along the radius of the gain medium is assumed when the numerical calculations were performed, however, there is some variations of the pump power distribution inside the gain medium in the experiments. The environmental perturbations also have some effects on the measured pulse sequences for each mode. The transverse mode profile also has effect on the antiphase states on the microchip lasers as discussed in Ref. [6], the two-pulse group of first-mode and second-mode in Fig. 4 may be caused the instability of the transverse mode, however, the total output pulse characteristics is not affected by this transverse mode instability. Although there are some simplifications in the numerical calculations, the numerical simulations of the antiphase states for the Cr,Yb:YAG self-Q-switched laser give us a clear image of the spatial hole burning of the gain medium and the nonlinear absorption of the saturable absorber on the dynamics of the antiphase states.

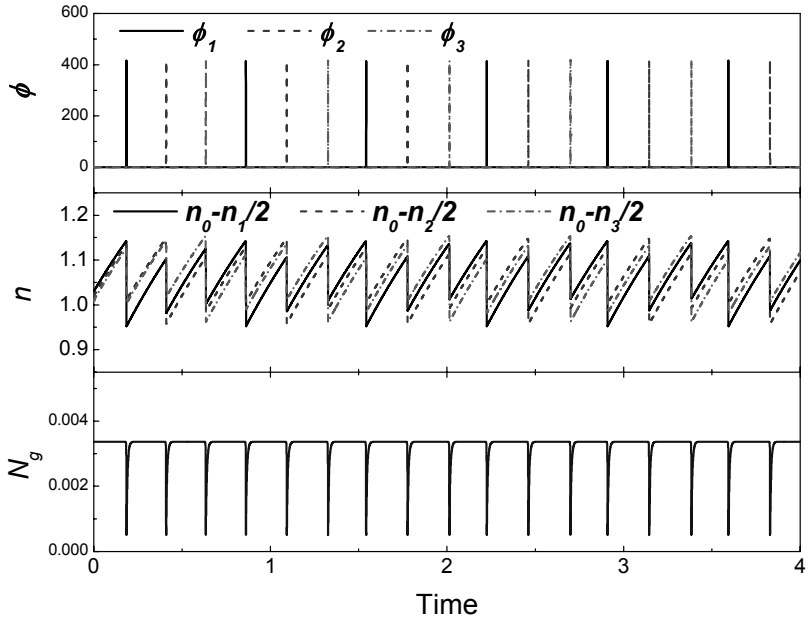

(a)

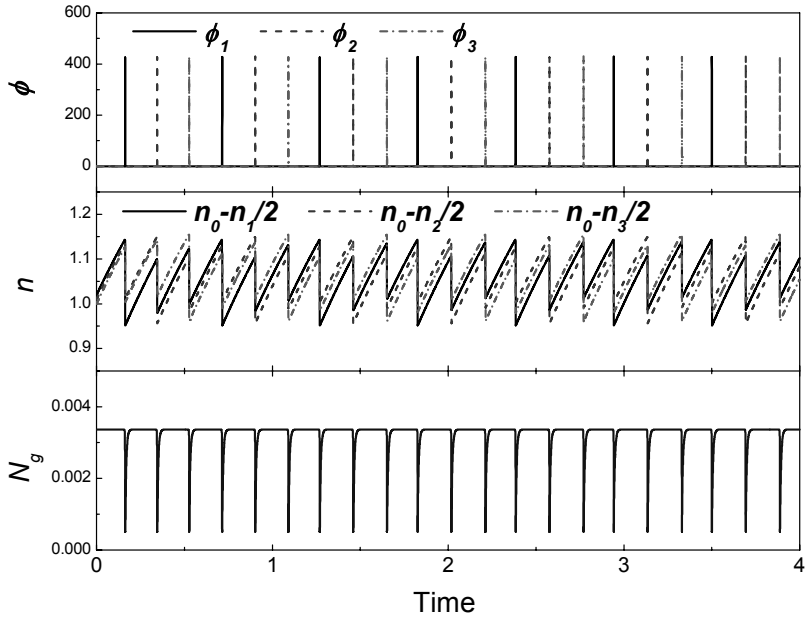

(b)

Figure 6: Numerical simulation of the pulse sequences, the population inversion of each mode and the population inversion of the saturable absorber for three-mode oscillation under different pump power ratio (a) $w = 1.7$, (b) $w = 1.85$.

4. CONCLUSIONS

In conclusions, the antiphase dynamics of laser-diode-pumped Cr,Yb:YAG microchip self-Q-switched laser were investigated experimentally and numerically. The stable two-mode and three-mode oscillation in Cr,Yb:YAG self-Q-switched lasers were observed in the wide pump range, the antiphase dynamics of this laser were investigated by separating the pulse sequences of each mode, the classical antiphase state of the two-mode oscillation and quasi-antiphase states of the three-mode oscillation were obtained experimentally. The numerical simulations based on the multimode passively Q-switched laser rate equations almost reproduced the observed antiphase dynamics of the two- and three-mode oscillation, and explained the antipahse dynamics of Cr,Yb:YAG self-Q-switched laser. The stable antiphase states in compact microchip Cr,Yb:YAG self-Q-switched laser will be a promising source for secure information encoding and transmission.

Acknowledgements: This work was supported by the 21st Century Center of Excellence (COE) program of Ministry of Education, Science and Culture of Japan. J. Dong would like to thank Prof. P. Deng of Shanghai Institute of Optics and Fine Mechanics, Chinese Academy of Sciences for providing the Cr,Yb:YAG samples.

REFERENCES

1. P. Hadley and M. R. Beasley, Appl. Phys. Lett. **50**, 621 (1987).
2. T. Baer, J. Opt. Soc. Am. B **3**, 1175 (1986).
3. K. Otsuka, Phys. Rev. Lett. **67**, 1090 (1991).
4. K. Otsuka, M. Georgiou, and P. Mandel, Jpn. J. Appl. Phys. **31**, L1250 (1992).
5. K. Otsuka, P. Mandel, M. Georgiou, and C. Etrich, Jpn. J. Appl. Phys. **32**, L318 (1993).
6. K. Otsuka, Jpn. J. Appl. Phys. **32**, L1414 (1993).
7. M. A. Larotonda, A. M. Yacomotti, and O. E. Martinez, Opt. Commun. **169**, 149 (1999).
8. Q. Zhang, B. Feng, D. Zhang, P. Fu, Z. Zhang, Z. Zhao, P. Deng, J. Xu, X. Xu, Y. Wang, and X. Ma, Opt. Commun. **232**, 353 (2004).
9. E. A. Viktorov and P. Mandel, Opt. Lett. **22**, 1568 (1997).
10. J. J. Zayhowski, J. Alloys Comp. **303-304**, 393 (2000).
11. J. Dong, P. Deng, Y. Liu, Y. Zhang, G. Huang, and F. Gan, Chin. Phys. Lett. **19**, 342 (2002).
12. J. J. Zayhowski and C. Dill-III, Opt. Lett. **19**, 1427 (1994).
13. A. A. Lagatsky, A. Abdolvand, and N. V. Kuleshov, Opt. Lett. **25**, 616 (2000).
14. G. J. Spuhler, R. Paschotta, M. P. Kullberg, M. Graf, M. Moser, E. Mix, G. Huber, C. Harder, and U. Keller, Appl. Phys. B **72**, 285 (2001).
15. J. Dong, A. Shirakawa, S. Huang, Y. Feng, K. Takaichi, M. Musha, K. Ueda, and A. A. Kaminskii, Laser Phys. Lett. **2**, 387 (2005).
16. J. Dong, M. Bass, Y. Mao, P. Deng, and F. Gan, J. Opt. Soc. Am. B **20**, 1975 (2003).
17. W. Kochner, *Solid State Laser Engineering* (Springer-Verlag, Berlin, 1999).
18. C. L. Tang, H. Statz, and G. Demars, J. Appl. Phys. **34**, 2289 (1963).
19. J. Dong and P. Deng, J. Lumin. **104**, 151 (2003).

* dong@ils.uec.ac.jp; phone: +81-0424-43-4708; Fax: +81-0424-85-8960.